Original Paper

phys. stat. sol. (b) **242**, No. 13, 2587–2594 (2005) / **DOI** 10.1002/pssb.200541090

Development and control of MOVPE growth processes for devices using reflectance anisotropy spectroscopy and normalized reflectance

Martin Zorn[*, 1] and **J.-Thomas Zettler**[2]

[1] Ferdinand-Braun-Institut für Höchstfrequenztechnik (FBH), Gustav-Kirchhoff-Str. 4, 12489 Berlin, Germany
[2] LayTec GmbH, Helmholtzstr. 13–14, 10587 Berlin, Germany

Received 22 June 2005, revised 16 August 2005, accepted 16 August 2005
Published online 21 September 2005

PACS 42.55.Px, 78.40.Fy, 78.66.Fd, 81.15.Gh, 85.30.Pq, 85.60.Jb

The use of the optical *in situ* techniques reflectance anisotropy (RA) and normalized reflectance (NR) for metal-organic vapour-phase epitaxy (MOVPE) growth processes of compound semiconductor devices is reviewed. The RA signal detects small deviations in the doping profile during growth of hetero-bipolar transistors and correlates to the emission wavelength of edge-emitting laser structure via its sensitivity to the quantum well composition. The NR signal is crucial for the alignment of distributed Bragg reflectors (DBR) in vertical-cavity surface-emitting lasers. With simultaneously performed RA and NR measurements the doping profile as well as the DBR alignment can be determined *in situ*. The composition monitoring in quaternary InGaAsP grown on InP is demonstrated using the RA signal for the As : P ratio while the NR signal is used for the Ga : In ratio. For AlGaInP on GaAs the NR signal is sensitive to both the aluminium and the indium content. Therefore these effects have to be separated via the determination of the growth efficiency of the respective materials using the growth rate calculated from the NR signal.

1 Introduction

Semiconductor devices like hetero-bipolar transistors (HBTs), vertical-cavity surface-emitting lasers (VCSELs) and edge-emitting lasers (EELs) are essential components not only in todays optical and wireless data transmission systems but also in a number of other applications like data storage and materials processing. Growth of layer structures for these devices on production scale is mainly done by metal-organic vapour-phase epitaxy (MOVPE) due to its high efficiency. To fulfil the stringent requirements on the final device a highly reproducible growth process is necessary. Parameters like the material composition or the doping profile in the grown layer structure define the properties of the finally resulting device. *In situ* measurements enable an early and efficient detection of these parameters already during the growth process [1]. Under gas-phase conditions only *optical in situ* techniques can be applied in contrast to e.g. molecular beam epitaxy (MBE) where the ultra-high vacuum (UHV) environment enables the application of reflection high-energy electron diffraction (RHEED).

This paper reviews the results of reflectance anisotropy spectroscopy (RAS [2]; also known as reflectance difference spectroscopy, RDS [3]) and normalized reflectance (NR, R/R_{Ref}) investigations in metal-organic vapour-phase epitaxy (MOVPE) for the development and fabrication of semiconductor devices. Processes and *in situ* measurements related to HBTs [4], EELs [5] as well as to VCSELs [6] are discussed. The possibility of controlling the composition even of quaternary materials such as InGaAsP [7] and AlGaInP [8] is highlighted in the last part of this paper.

[*] Corresponding author: e-mail: martin.zorn@fbh-berlin.de, Phone: +49 30 6392 2676, Fax: +49 30 6392 2685

2 Experimental

The results which are reviewed here are obtained in Aixtron 200 and Aixtron 200/4 low-pressure metal-organic vapour-phase epitaxy (MOVPE) reactors. *In situ* investigations in planetary reactors are not presented here but can be found e.g. in Refs. [9] and [10]. The source materials used include trimethylgallium (TMGa), trimethylaluminum (TMAl), trimethylindium (TMIn), arsine (AsH_3) and phosphine (PH_3). Dopants used were Si from Si_2H_6 for n-type, and Zn from diethylzinc (DEZn), extrinsic carbon doping using carbontetrabromide (CBr_4) or intrinsically incorporated carbon by growth at low V/III ratios for p-type, respectively. A typical growth temperature was 770 °C. The MOVPE systems are equipped with strain free, UV transparent viewports for normal incidence optical access and with a corresponding hole in the liner-tube. LayTec EpiRAS spectrometers have been used in all cases giving the possibility of performing reflectance anisotropy measurements also on rotating samples [11].

RAS measurements are highly sensitive to the optical anisotropy induced by the surface reconstruction. RAS measures the complex difference in reflectance for linear polarized light along the two principal axis on the surface. For a (001) surface the RAS signal is given by

$$\frac{\Delta r}{r} = \mathrm{Re}\left(\frac{\Delta r}{r}\right) + i \cdot \mathrm{Im}\left(\frac{\Delta r}{r}\right),$$
$$\frac{\Delta r}{r} = 2\,\frac{r_{[\bar{1}10]} - r_{[110]}}{r_{[\bar{1}10]} + r_{[110]}}. \qquad (1)$$

In (1) $r_{[110]}$ and $r_{[\bar{1}10]}$ are the complex reflectances of light polarized linearly along the indicated directions in the surface (see [1] for details). Please note that all spectra are taken on rotating samples. Therefore all viewgraphs show the absolute values of the real part of the RA signal.

The reflectance $R = r \cdot r^* = |r|^2 = I_r/I_i$ is by definition the ratio between the reflected light intensity I_r and the incident intensity I_i. When R is measured *ex situ*, usually beam-splitting techniques are applied for detecting both I_i and I_r synchronously. For *in situ* measurements, influenced e.g. by varying window absorbance, this is not feasible. Therefore, we used the normalized reflectance R/R_{ref}, which is the actual reflectance of the growing layer stack divided by the reflectance of a well known reference sample inside the reactor. In this work the GaAs substrate reflectance $R_{\mathrm{ref}} = R_{\mathrm{GaAs}}$ was measured prior to the growth of the epitaxial structure and used thereafter as reference. The normalized reflectance can furthermore be simulated by a multilayer growth model based on a high-temperature dielectric function database. In addition, similarly and complementarily to RAS, the normalized reflectance R/R_{ref} can be directly used for the comparison of growth processes in different growth systems.

3 Results and discussion

3.1 Monitoring of complete growth processes

The MOVPE growth process of complete device structures includes the epitaxy of up to 200 different layers depending on the purpose of the final device. Therefore the continuously measured RA and NR spectra are usually color-coded [4] in order to display the fully 4-dimensional measurement (RAS, R/R_{ref}, growth time, wavelength, see, e.g., Figs. 1 and 3). The resulting diagrams give a distinctive fingerprint of the entire growth process since the RA signal is sensitive to the important layer properties like the doping concentration [12, 13] of the respective layer and the reflectance gives access to growth rate and layer composition. Figure 1a shows a RA color-plot taken during a complete growth run for a HBT device [4]. The different materials (GaAs and InGaP in this case) with their different doping concentration can clearly be distinguished. To compare different growth runs Figs. 1b and c show the difference to the reference color-plot of growth run ‘a’ where green indicates no differences while red indicates differences in the growth process. As it is clearly visible in Fig. 1b there is a difference in the doping of layer #6 (p-GaAs). The response in the RA signal is due to an intended change of the doping concentration in this layer from 3×10^{19} to 1×10^{19}. The growth run represented in Fig. 1c shows no difference as com-

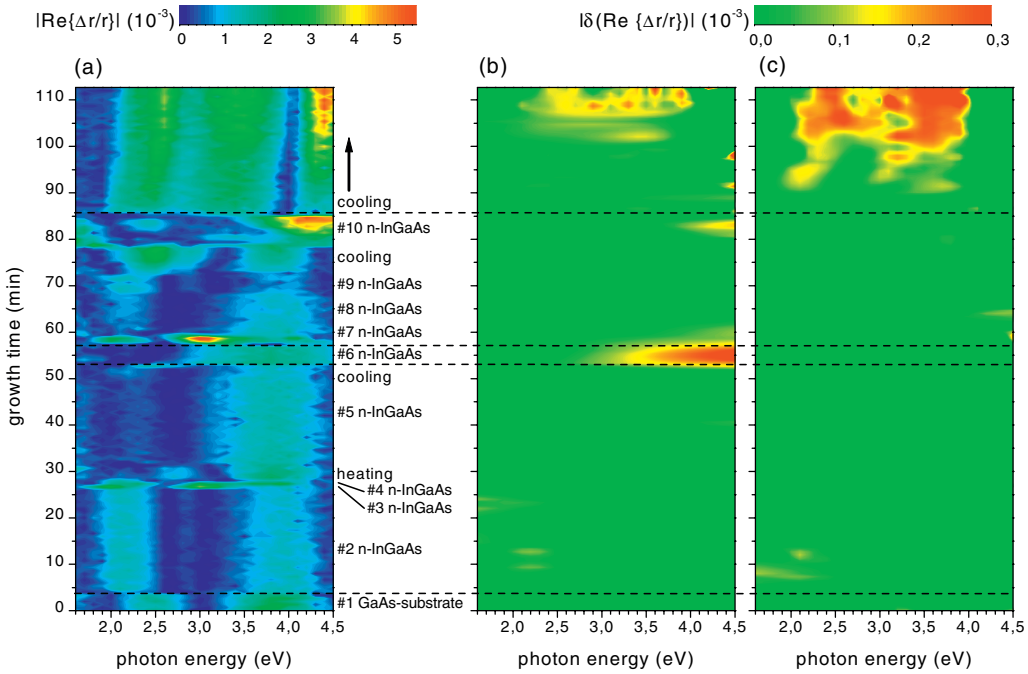

Fig. 1 (online colour at: www.pss-b.com) a) RA color-plot of the growth process for a HBT layer structure. The data in b) and c) from two subsequent HBT growth processes show the difference to the data from the growth run shown in a). Green indicates no difference to HBT a. In b) the doping of layer #6 was reduced from 3×10^{19} to 1×10^{19} whereas HBT (c) was grown under nominally the same conditions as HBT (a) (figure taken from Ref. [4]).

pared to that of Fig. 1a. This shows the good reproducibility of the growth process. Only the cooling behaviour after growth was different due to a differently covered liner tube.

Differences in composition or doping concentration in principle result in changes over the whole spectral range of the RA measurement. However, there are spectral regions where this change is more pronounced. For example from Fig. 1b it can be seen that the strongest difference in the RA signal is at higher photon energies. This is the same in the AlGaAs case, where the strongest signal response to doping changes can be found around 3.8 eV [5, 6]. This is advantageous for the response time since the penetration depth of the light decreases with increasing photon energy. At 3.8 eV for example the penetration depth of the light into the AlGaAs layers is in the range of only 10 nm. Therefore a transient single wavelength measurement at this wavelength which has a much higher time resolution than the spectral color-plot measurement can be very useful to even resolve thin layers like quantum wells (QW). Figure 2 shows the time-resolved measurements of three NIR-laser structures. A corresponding RA fingerprint can be found in Ref. [5]. They consist of a GaAsP QW embedded in $Al_{0.5}Ga_{0.5}As$ waveguide and $Al_{0.7}Ga_{0.3}As$ cladding layers (see Ref. [14] for details). Comparing both cladding layers consisting of n- and p-doped $Al_{0.7}Ga_{0.3}As$ the clear difference in the RA value at 3.8 eV can be seen. Comparing the cladding and the waveguide layer on both sides of the QW a strong shift in the RA caused by the different aluminium content is visible. A strong increase in the RA values over the whole spectral range is reported with increasing Al content [15]. However, this effect is superposed by an additional change in the RA signal caused by a change in doping concentration between cladding and waveguide layers. Comparing the RA measurements of the waveguide layers ($Al_{0.5}Ga_{0.5}As$) on both sides of the QW a decrease of the n-doping concentration on the left side towards the QW followed by an increase of the doping concentration towards the p-waveguide layer on the right side is clearly visible. This doping profile is a crucial parameter determining the performance of the final laser diode. Comparing the three transients a high reproducibility of the growth process as well as of the RAS measurement can be stated. Small deviations in the growth process (especially in composition or doping concentration) would be

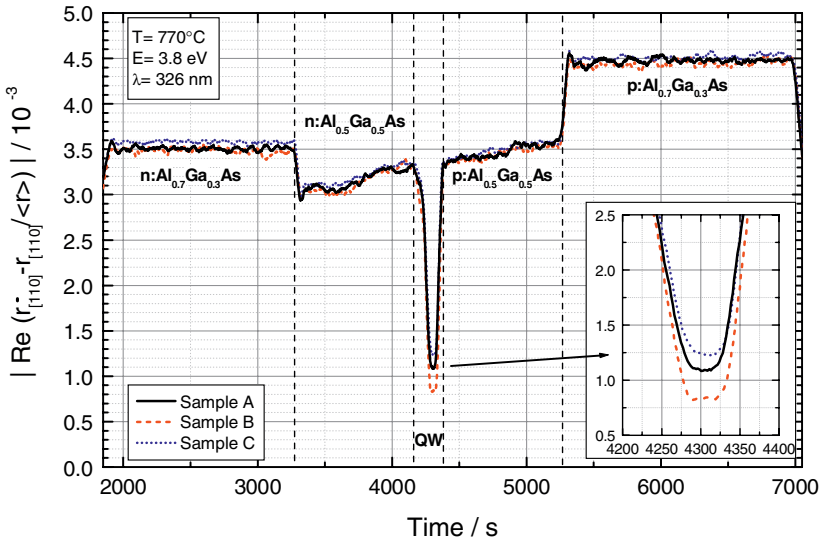

Fig. 2 (online colour at: www.pss-b.com) RA transients showing cladding, waveguide and QW layers of three different growth runs for edge-emitting laser structures taken at 3.8 eV and 770 °C growth temperature. The three structures have the same cladding and waveguide layers and differ only in the QW region. The inset shows a magnification of the RA transient during QW growth resulting in different emission wavelength via a different As : P ratio in the GaAsP-QW (figure taken from Ref. [5]).

detected easily in such transients. When comparing the three transients during growth of the QW (see inset) a difference shows up. This is caused by a different As:P ratio in the GaAsP-QW resulting in different emission wavelength of the laser diode. In detailed investigations a correlation between the RA level during the QW growth and the photoluminescence emission wavelengths of the QW could be established [5] based on the known strong dependence of the RA signal around 2.5 eV and 3.8 eV on the GaAsP composition [16, 17].

For the growth of VCSEL structures it has been shown that the measurement of the visible reflectance is needed for the alignment of the n : DBR, p : DBR and the cavity [6] and can additionally be used for the determination of interface roughness in the whole structure [18]. Furthermore it has been shown, that also the UV reflectance anisotropy is very helpful for the control of the doping levels [6]. The most comprehensive *in situ* access to this kind of process would be to measure both optical properties (UV-RA and visible NR) at the same time. For this purpose an EpiRAS sensor was applied together with a fibre-coupled EpiR-MF sensor to measure both signals *simultaneously* in the two different wavelength ranges. Figure 3 shows the measurement of a VCSEL structure consisting of 25 n : DBR pairs and 15.5 p : DBR pairs sandwiching the AlGaInP cavity containing three GaInP QWs. The left side (Fig. 3a) shows the normalized reflectance in the wavelength range between 620 nm and 775 nm while the right side (Fig. 3b) shows the simultaneous measured reflectance anisotropy at 3.8 eV. From this measurement a good alignment of the DBR mirrors and the cavity (see Fig. 8 in Ref. [6] for comparison) together with the doping profile of the whole structure can nicely be seen. Due to the known dependence of the RA signal on doping type and concentration for AlGaAs [5] as well as for AlGaInP [19] the RA signal resolves the doping profile of the DBR and cavity layers together with the three QWs. More details on the growth process and the final performance of the VCSEL devices can be found in Refs. [20] and [21].

3.2 Composition control

A direct control of the composition in ternary and quaternary materials would be very helpful since the composition defines important layer properties like the emission wavelength or the strain state of the respective layer. Real composition control using ellipsometry has been reported by a direct control of the

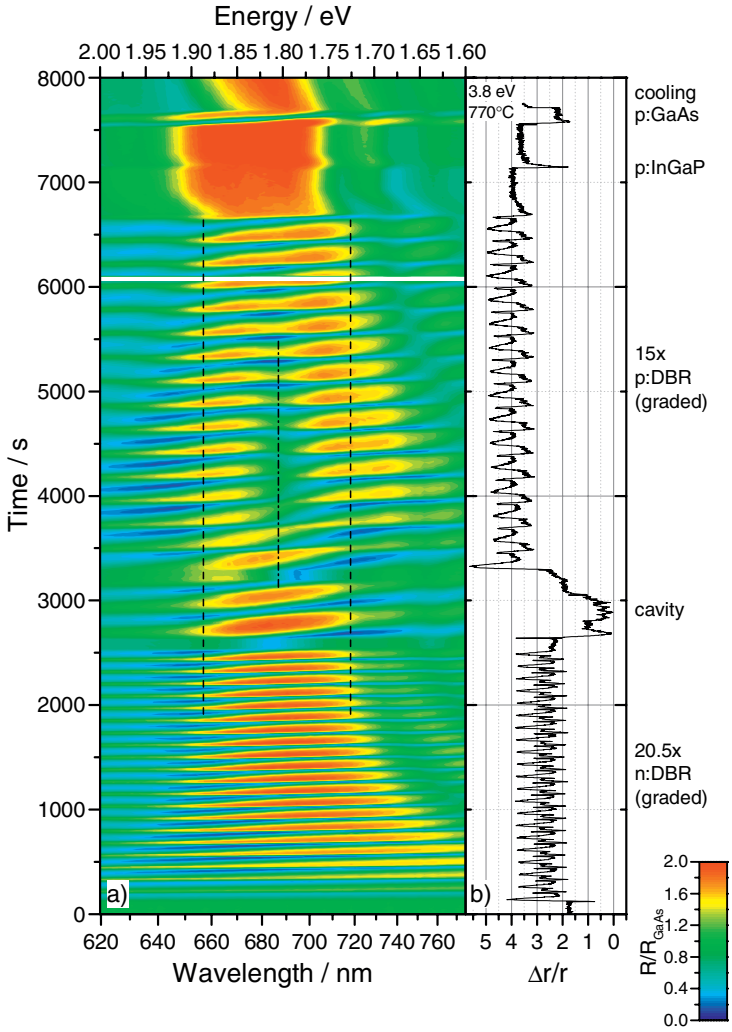

Fig. 3 (online colour at: www.pss-b.com) Simultaneous measurement of the visible normalized spectral reflectance R/R_{GaAs} (a) and the reflectance anisotropy at 3.8 eV (b) during growth of a VCSEL structure at 770 °C for an emission wavelength of 650 nm.

TMIn mass flow controller (MFC) via the ellipsometry computer for the growth of InGaAs on InP [22] and InGaP on GaAs [23]. However, the application of an ellipsometer at a MOVPE system is much more difficult due the large angle of incidence and the extreme alignment sensitivity as compared to the normal-incidence RA and NR techniques [24].

In laser diodes for telecommunication applications in the 1.3 μm to 1.55 μm range InP and quaternary $In_{1-x}Ga_xAs_{1-y}P_y$ are used as material for the different layers in the device structures. For lattice matched growth which is required to grow for example thick strain and defect free waveguide layers both compositions (indium x) and (arsenic y) have to be adjusted carefully [7]. The sum of the surface sensitive RAS signals at 1.75 eV and 2.65 eV associated with the phosphorus to arsenic ratio was used to evaluate predominantly the composition parameter y while access to the composition parameter x was established through the normalized *in situ* measured growth rate. With the help of the combined RA/NR *in situ* calibration the need of test growth runs could significantly be reduced. In this case the high sensitivity of the RA signal to the As:P ratio in the layers is exploited as also reported for GaAsP [16, 17]. For the Ga:In ratio the following effect is used: An increasing Ga content of the respective quaternary layers

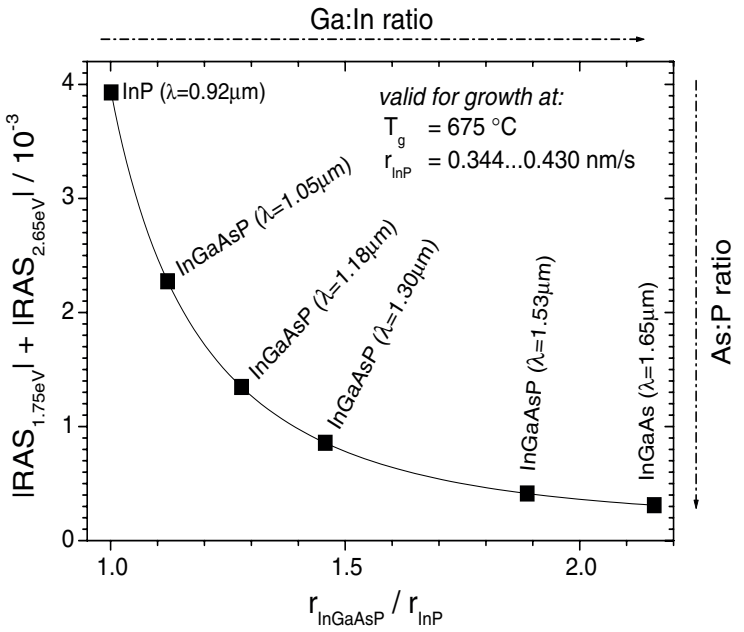

Fig. 4 Calibration curve gained from the calibration of the As : P and the Ga : In ratio for the growth of InGaAsP on GaAs (figure taken from Ref. [7]).

causes an increase in the average reflectance and a decreasing period time of the Fabry–Perot oscillations due to a higher growth rate. To use this effect for an *in situ* calibration routine the TMIn flux has to be kept constant while the TMGa flux was varied. Therefore, the change in growth rate is then a direct measure for the Ga : In ratio in the layer. Combining the RA (RA taken at 1.75 eV + RA taken at 2.65 eV) and the NR response ($r_{InGaAsP}/r_{InP}$) of the calibration leads to a full control of the composition to a targeted emission wavelength. The resulting calibration diagram is displayed in Fig. 4.

For GaAs-based laser diodes emitting in the red region (around 650 nm) $(Al_xGa_{1-x})_{0.52}In_{0.48}P$ has to be grown lattice matched to GaAs. In contrast to $In_xGa_{1-x}As_yP_{1-y}$ which consists of two group III and two group V components $(Al_xGa_{1-x})_{0.52}In_{0.48}P$ consists of three group III components and only one group V component. Figure 5a shows the dependence of the RA signal on the aluminium content x in $(Al_xGa_{1-x})_{0.52}In_{0.48}P$ for x = 0, 0.2, 0.5, 0.7 and 1 at 700 °C. A clear change in the amplitude as well as in the energetic position of the main peak around 3 to 3.5 eV can be seen. As it has already been shown, this composition dependence correlates to the dependence of the E_1 feature in the band structure [19].

The disadvantage of the RA measurement (which is usually its advantage) is the additional sensitivity of the RA signal to other layer properties and surface conditions (e.g. phosphorus coverage and doping level). Therefore the absolute composition determination should be based on a bulk related effect like the reflectance R. Figure 5b shows NR transients taken at 3.5 eV during growth of a test structure consisting of three differently strained very thin (12 nm) $Al_{1-y}In_yP$ layers. Growth of the respective $Al_{1-y}In_yP$ layers was stopped after the first half of the Fabry–Perot interference to minimize the incorporated strain and suppress formation of defects. As it can be seen the amplitude of the minimum clearly correlates to the indium content of the layer.

For a real composition control two ways are proposed: The first way is to start with the aluminium composition x. This value can be calibrated independently by growing $Al_xGa_{1-x}As$ layers as demonstrated earlier [25], since the aluminium to gallium ratio is similar for $Al_xGa_{1-x}As$ and $(Al_xGa_{1-x})_{0.52}In_{0.48}P$. This well known aluminium composition should then be used for the growth of $(Al_xGa_{1-x})_{0.52}In_{0.48}P$ with the desired x value. The y value can then be determined by reflectance measurements on test structures using $(Al_xGa_{1-x})_{1-y}In_yP$ layers with varying y. Due to the high sensitivity of the UV reflectance measurement these layers can be grown very thin giving the possibility to grow several of these layers in one single

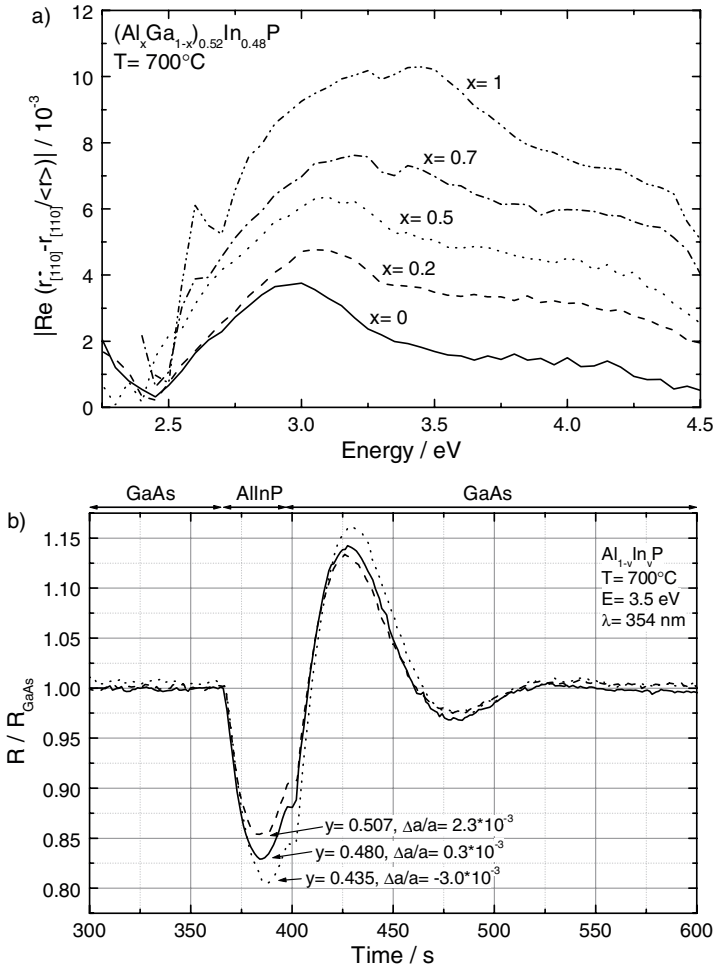

Fig. 5 a) Dependence of spectral RA signal on aluminium content x in $(Al_xGa_{1-x})_{0.52}In_{0.48}P$ at 700 °C. b) NR transients (R/R_{GaAs}) of thin $Al_{1-y}In_yP$ layers embedded in GaAs taken at 3.5 eV and 700 °C growth temperature (figures taken from Ref. [8]).

test structure. For the second approach first the indium content y is adjusted for the two ternary materials $Ga_{1-y}In_yP$ and $Al_{1-y}In_yP$ according to the method described in Fig. 5b. Finally the gallium-to-aluminium ratio is *in situ* calibrated using interpolation schemes based on the known dependence of the growth efficiency on the aluminium content x [8].

4 Summary

RAS shows a high sensitivity to important layer parameters like doping concentration and composition when applied to compound semiconductor device growth in MOVPE. This makes it a very helpful tool for the development and fabrication of device structures. The reproducibility of the growth process can for example be controlled by an easy detection of deviations in the growth process as compared to a reference sample. Furthermore it could be shown that also the normalized reflectance is a very helpful measurement for the determination of the growth rate and the alignment of DBR mirrors and the cavity resonance in a VCSEL structure.

The *in-situ* composition determination of quaternary materials is difficult due to compensation effects between strain and composition contribution to the optical signals. However, recent detailed studies

showed that it is possible to calibrate even the growth of the quaternary materials InGaAsP and AlGaInP with combined RA and NR measurements.

Acknowledgments The authors would like to thank K. Haberland, P. Wolfram, E. Steimetz and W. Ebert for the possibility to show their measured data in this review article and M. Weyers for critical reading the manuscript. Part of this work was supported under grant WF-3203 (Innovationsförderprogramm, financed by the City of Berlin and European fond for regional development).

References

[1] J.-T. Zettler, K. Haberland, M. Zorn, M. Pristovsek, W. Richter, P. Kurpas, and M. Weyers, J. Cryst. Growth **195**, 151 (1998).
[2] M. Zorn, J. Jönsson, W. Richter, J.-T. Zettler, and K. Ploska, phys. stat. sol. (a) **152**, 23 (1995).
[3] D. E. Aspnes, Mater. Sci. Eng. B **30**, 109 (1995).
[4] K. Haberland, P. Kurpas, M. Pristovsek, J.-T. Zettler, M. Weyers, and W. Richter, Appl. Phys. A **68**, 309 (1999).
[5] M. Zorn and M. Weyers, J. Cryst. Growth **276**, 29 (2005).
[6] M. Zorn, K. Haberland, A. Knigge, A. Bhattacharya, M. Weyers, J.-T. Zettler, and W. Richter, J. Cryst. Growth **235**, 25 (2002).
[7] P. Wolfram, E. Steimetz, W. Ebert, N. Grote, and J.-T. Zettler, J. Cryst. Growth **272**, 118 (2004).
[8] M. Zorn, J.-T. Zettler, A. Knauer, and M. Weyers, J. Cryst. Growth (2005), in print.
[9] N. Habets, T. Schmitt, M. Deufel, M. Lünenbürger, M. Heuken, and H. Jürgensen, Thin Solid Films **409**, 43 (2002).
[10] T. Bergunde, B. Henninger, M. Lünenbürger, M. Heuken, M. Weyers, and J.-T. Zettler, J. Cryst. Growth **248**, 235 (2003).
[11] K. Haberland, O. Hunderi, M. Pristovsek, J.-T. Zettler, and W. Richter, Thin Solid Films **313–314**, 620 (1998).
[12] H. Tanaka, E. Colas, I. Kamiya, D. E. Aspnes, and R. Bhat, Appl. Phys. Lett. **59**, 3443 (1991).
[13] M. Pristovsek, S. Tsukamoto, N. Koguchi, B. Han, K. Haberland, J.-T. Zettler, W. Richter, M. Zorn, and M. Weyers, phys. stat. sol. (a) **188**, 1423 (2001).
[14] J. Sebastian, G. Beister, F. Bugge, F. Buhrandt, G. Erbert, H. G. Hänsel, R. Hülsewede, A. Knauer, W. Pittroff, R. Staske, M. Schröder, H. Wenzel, M. Weyers, and G. Tränkle, IEEE J. Sel. Top. Quantum Electron. **7**, 334 (2001).
[15] K. C. Rose, S. J. Morris, D. I. Westwood, D. A. Woolf, R. H. Williams, and W. Richter, Appl. Phys. Lett. **66**, 1930 (1995).
[16] J. Jönsson, F. Reinhardt, M. Zorn, K. Ploska, W. Richter, and J. Rumberg, Appl. Phys. Lett. **64**, 1998 (1994).
[17] M. Zorn, J. Jönsson, A. Krost, W. Richter, J.-T. Zettler, K. Ploska, and F. Reinhardt, J. Cryst. Growth **145**, 53 (1994).
[18] K. Haberland, M. Zorn, A. Klein, A. Bhattacharya, M. Weyers, J.-T. Zettler, and W. Richter, J. Cryst. Growth **248**, 194 (2003).
[19] K. Haberland, A. Bhattacharya, M. Zorn, M. Weyers, J.-T. Zettler, and W. Richter, J. Electron. Mater. **29**, 468 (2000).
[20] M. Zorn, A. Knigge, U. Zeimer, A. Klein, H. Kissel, M. Weyers, and G. Tränkle, J. Cryst. Growth **248**, 186 (2003).
[21] A. Knigge, M. Zorn, M. Weyers, and G. Tränkle, Electron. Lett. **38**, 882 (2002).
[22] T. Trepk, M. Zorn, J.-T. Zettler, M. Klein, and W. Richter, Thin Solid Films **313–314**, 496 (1998).
[23] M. Zorn, T. Trepk, P. Kurpas, M. Weyers, J.-T. Zettler, and W. Richter, J. Cryst. Growth **195**, 223 (1998).
[24] J.-T. Zettler, T. Wethkamp, M. Zorn, M. Pristovsek, C. Meyne, K. Ploska, and W. Richter, Appl. Phys. Lett. **67**, 3783 (1995).
[25] K. Haberland, A. Kaluza, M. Zorn, M. Pristovsek, H. Hardtdegen, M. Weyers, J.-T. Zettler, and W. Richter, J. Cryst. Growth **240**, 87 (2002).